Materials Chemistry and Physics xxx (2012) 1–6

Contents lists available at SciVerse ScienceDirect

Materials Chemistry and Physics

journal homepage: www.elsevier.com/locate/matchemphys

The role of Ni content on the stability of Cu–Al–Ni ternary alloy in neutral chloride solutions

H. Nady [b], N.H. Helal [b], M.M. El-Rabiee [b], W.A. Badawy [a,*]

[a] Chemistry Department, Faculty of Science, Cairo University, 12 613 Giza, Egypt
[b] Chemistry Department, Faculty of Science, Fayoum University, Fayoum, Egypt

ARTICLE INFO

Article history:
Received 19 May 2011
Received in revised form
5 March 2012
Accepted 22 March 2012

Keywords:
Cu–Al–Ni alloys
Corrosion
Impedance
Passivation
Polarization

ABSTRACT

The effect of systematic increase of Ni content on the electrochemical behavior of the Cu–Al–Ni ternary alloys in neutral chloride solutions was investigated. Alloys with Ni contents, 5, 10, 30 and 45 mass% were used. The effect of chloride ions on the electrochemical behavior of these alloys was investigated. The presence of Al in the alloy increases its stability. An increase in the nickel content decreases the corrosion rate of the alloys. Conventional electrochemical techniques and electrochemical impedance spectroscopy, EIS, were used. The impedance measurements have shown that the increase of the Ni content and the immersion time of the alloys in the chloride solution increase the corrosion resistance of the alloys. The experimental impedance data were fitted to theoretical data according to a proposed model representing the electrode/electrolyte interface and the equivalent circuit parameters were calculated.

1. Introduction

The Cu–Ni alloys possess attractive mechanical properties, high thermal and electrical conductivities and good corrosion resistance in a variety of environments at moderately elevated temperatures (60–80 °C) [1–3]. The addition of aluminum to these binary alloys improves the light weight of the alloy and increases its corrosion resistance, especially in seawater, sulfuric acid and salt solutions [3–6]. It provides good wear properties, better workability and resistance to high temperature oxidation [4–6]. The good corrosion resistance of the Cu–Al–Ni alloys is due to the formation of a protective layer of alumina, which builds up quickly on the surface post-exposure to the corrosive environment [6–8]. The passivation of the alloy is based on the fact that aluminum has a greater affinity toward oxygen than copper and considerable stability of Al_2O_3 than Cu_2O in neutral solutions [9,10]. The essential role of Ni in the passivation of Cu–Ni alloys has been attributed to its incorporation into the Cu (I) oxide which is formed as corrosion product during the corrosion of the alloy [11,12]. The incorporation of nickel ions reduces the number of cation vacancies that normally exist in Cu (I) oxide. The substitution of Ni in the Cu (I) oxide increases with the increase in the Ni content of the alloy at least up to 30% [13]. Copper/nickel alloys have tremendous applications in different industries, where chloride containing water are always used.

The understanding of the electrochemical behavior of these alloys in the presence of chloride ions together with the control of the factors that govern the stability of the alloys in corrosive environments an important subject worthy of intensive investigations. Cu–Ni alloys have been widely studied in NaCl solutions with contradictory results; some authors [14,15] have found that selective removal of nickel is predominant, whereas others [16,17] have suggested that the de-alloying of copper is the main process. Nickel additions in excess of around 30% resulted in a passivation of copper alloys in chloride solutions [18]. The reason for this belief was related to simplified calculations, which show that the 'd' shell should become unfilled at around this nickel content. The corrosion rate of the binary Cu–Ni alloys with different Ni contents was found to decrease with the increase in nickel content and to increase with the increase of chloride concentration up to 0.3 mol dm^{-3}. At higher concentrations of chloride ions ($[Cl^-] > 0.3$ mol dm^{-3}) the corrosion rate was found to decrease [19].

In this paper we are aiming at the understanding of the effect of Ni content on the electrochemical behavior of the ternary Cu–Al–Ni alloy in neutral chloride solutions. It is essential to clarify the fundamentals of the corrosion mechanism and passivation processes taking place at the alloy/solution interface and the role of chloride ions in this aspect. The systematic increase of the Ni

* Corresponding author. Tel.: +2 02 3567 6558; fax: +2 02 35685799.
E-mail addresses: wbadawy@cu.edu.eg, wbadawy50@hotmail.com (W.A. Badawy).

0254-0584/$ – see front matter © 2012 Elsevier B.V. All rights reserved.
doi:10.1016/j.matchemphys.2012.03.096

content and the chloride ion concentration will be investigated and discussed. In this respect, different electrochemical techniques, e.g. open-circuit potential measurements, polarization techniques and electrochemical impedance spectroscopy, EIS, were used. The experimental impedance data were fitted to theoretical data according to an equivalent circuit model simulating the electrode/electrolyte interface. The alloy surface was analyzed by x-ray dispersive analysis, EDX.

2. Experimental details

The working electrodes were made from commercial grade Cu–Al–Ni rods, mounted into glass tubes by two-component epoxy resin leaving a surface area of 0.2 cm^2 to contact the solution. The mass spectrometric analysis of the electrodes used is presented in Table 1. The relatively high iron percent ($\approx$2.2%) in the ternary Cu–10Al–5Ni and the Cu–10Al–10Ni alloys did not show remarkable effect on the behavior of the alloy. The surface analysis did not show any contribution of Fe to the barrier layer [20]. The electrochemical cell was a three-electrode all-glass cell, with a platinum spiral counter electrode and saturated calomel, SCE, reference electrode. Before each experiment, the working electrode was ground using successive grades emery papers down to 2000 grit. The electrode was washed thoroughly with distilled water, and transferred quickly to the cell. The electrochemical measurements were carried out in a stagnant, naturally aerated neutral chloride solution (0.6 mol dm^{-3} NaCl of pH 7.0).

The polarization experiments and electrochemical impedance spectroscopic investigations were performed using a Voltalab PGZ 100 "All-in-one" potentiostat/Galvanostat. The potentials were measured against and referred to the standard potential of the SCE (0.245 V vs. the standard hydrogen electrode, SHE). The polarization experiments were carried out using a scan rate of 5 mV s^{-1} in the potential range −550 to +150 mV. All cyclic voltammetry measurements were carried out using a scan rate of 10 mV s^{-1} in the potential range −800 to +200 mV. The scan rate was selected after measurements in the range 2 mV s^{-1} to 250 mV s^{-1} to avoid large electrochemical and chemical dissolution process at $\upsilon < 5$ mV s^{-1} or loss in the definition of different oxidation process at $\upsilon > 50$ mV s^{-1} [21]. The potential range was chosen to record any cathodic step that could be present before any anodic dissolution. The total impedance, Z, and phase shift, θ, were measured in the frequency range from 0.1 to 10^5 Hz. The superimposed ac-signal amplitude was 10 mV peak to peak. To achieve reproducibility, each experiment was carried out at least twice.

3. Results and discussion

3.1. Open-circuit potential measurements

The open-circuit potentials of the Cu–Al–Ni alloys with different Ni contents (5, 10, 30 and 45 mass% Ni) were traced over 1 h in the neutral chloride solution. The steady state potential of all alloys shift to less negative values as the Ni content increases (Fig. 1a). This means that the increase of the Ni content passivates the alloy surface leading to the noble shift in its OCP. The steady-state potential for all electrodes was reached within a maximum of 30 min from electrode immersion in the electrolyte. The Cu–10Al–45Ni shows an increase in the electrode potential in the few minutes from electrode immersion then decreases again until it reaches the steady state after 30 min. This behavior is more likely similar to the passivation effects of Ni, since the electrode surface is Ni rich and hence the passive behavior is recorded in the first 30 min of electrode immersion in the chloride solution [20,22]. This behavior was also confirmed by the impedance measurements. In all investigated alloys, the ratio of Al is constant which means that the extra passivation effect can be attributed to the increase in the Ni content.

Table 1
Mass spectrometric analysis for the different Cu–Al–Ni alloys in mass%.

Sample	Cu	Al	Ni	Zn	Mn	Sn	Fe	Si	Mg	Ti
Cu–Al–5Ni	81.16	11.15	4.98	0.11	0.02	0.14	2.22	0.21	0.01	–
Cu–Al–10Ni	76.00	11.28	9.95	0.10	0.02	0.14	2.26	0.24	0.01	–
Cu–Al–30Ni	60.02	9.32	29.17	0.08	0.01	0.13	1.10	0.16	0.01	–
Cu–Al–45Ni	43.31	9.56	46.01	–	–	0.04	0.72	0.35	–	0.01

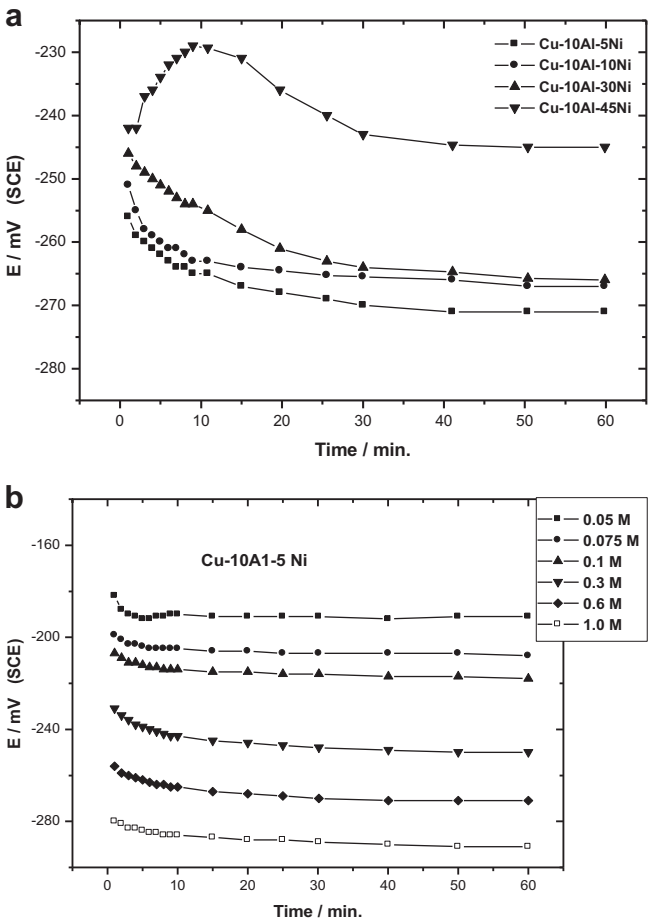

Fig. 1. a: Variation of the open-circuit potential of the different Cu–Al–Ni alloys with time in stagnant naturally aerated 0.6 mol dm^{-3} chloride solution of pH 7.0 at 25 °C. b: Effect of chloride ion concentration on the open-circuit potential of the Cu–10Al–5Ni alloy in stagnant naturally aerated neutral chloride solution at 25 °C.

The open-circuit potential of the Cu–Al–5Ni alloy in neutral solutions of different chloride ion concentrations (0.05–1.0 mol dm^{-3}) was also recorded over 1 h. The steady state potential of the alloy is reached within 15 min from electrode immersion in the different chloride solutions. The OCP of the alloy shifts toward negative values with the increase of the chloride ion concentration as presented in Fig. 1b. The increase of the concentration of the aggressive chloride ions leads to the attack of the barrier layer and decreases the passivity of the alloy surface and the potential shifts to more active values.

3.2. Cyclic voltammetry measurements

The cyclic voltammograms of the Cu–Al–Ni alloys with different Ni contents were recorded at a scan rate of 10 mV s^{-1} in a stagnant naturally aerated neutral 0.6 mol dm^{-3} chloride solution

Please cite this article in press as: H. Nady, et al., The role of Ni content on the stability of Cu–Al–Ni ternary alloy in neutral chloride solutions, Materials Chemistry and Physics (2012), doi:10.1016/j.matchemphys.2012.03.096

at 25 °C and presented in Fig. 2. The potential scan was initiated at −0.8 V where a transition region, in which the current density stabilizes with potential, was recorded, before the active metal dissolution occurs. This transition region is most probably due to the formation of adsorbed $CuCl^-_{ads}$ species on the electrode surface via a reaction [23]:

$$CuCl + e \rightarrow Cu + Cl^- \ [E^\circ = -0.085 \text{ V vs SHE}] \ [7]$$

$$Cu + Cl^- \rightarrow CuCl^-_{ads} \quad (1)$$

The adsorbed $CuCl^-_{ads}$ species are transformed into a porous CuCl film [24]. In the anodic region, the current density increases rapidly with increasing potential due to the formation of the soluble $CuCl^-_2$ either from the adsorbed layer or the copper on the alloy surface according to [2]:

$$CuCl + Cl^- \rightarrow CuCl^-_2 \quad (2)$$

$$Cu + 2Cl^- \rightarrow CuCl^-_2 + e^- \quad (3)$$

It was suggested that the presence of $CuCl^-_2$ at the metal surface leads to a hydrolysis reaction and the formation of Cu_2O [25,26] according to:

$$2CuCl^-_2 + H_2O \rightarrow Cu_2O + 4Cl^- + 2H^+ \quad (4)$$

The formation of the Cu_2O as an insoluble passive layer explains the decrease of the anodic current density. In the reverse scan, a clear cathodic peak appears at ~−250 mV due to the reduction of copper ions. However, the value of the dissolution current density and consequently the cathodic current density decreases with increasing the Ni content. As can be seen from the figure, the presence of ≥30% Ni decreases the corrosion current density as will be discussed later.

3.3. Potentiodynamic measurements

The values of the corrosion parameters i.e. the corrosion current density, i_{corr}, corrosion potential, E_{corr}, anodic and cathodic Tafel slopes were calculated from the potentiodynamic polarization data obtained for the different alloys in the stagnant naturally aerated neutral 0.6 mol dm^{-3} chloride solution and presented in Table 2. The potentiodynamic polarization curves are presented in Figs. 3 and 4. It is worthwhile to mention that the recorded corrosion potentials are more positive than the open circuit-potential. A difference of about 200 mV was recorded which was attributed to a prepassivation step [22,27]. Fig. 3 presents the potentiodynamic polarization curves of the different alloys in the stagnant naturally aerated neutral 0.6 mol dm^{-3} chloride solution. The corrosion rate was evaluated as function of the Ni content and a decrease in the corrosion rate with the increase of the Ni content was recorded. The decrease in the corrosion rate can be attributed to the incorporation of Ni ions in the mobile vacancies of the Cu_2O film decreasing the possibility of Cu dissolution from the alloy surface.

Table 2
Potentiodynamic polarization parameters of the different Cu–Al–Ni after 1 h of alloy immersion in stagnant naturally aerated 0.6 mol dm^{-3} chloride solution of pH 7.0 at 25 °C.

Alloys	E_{corr}/mV	i_{corr}/μA/cm^2	β_a/mV	β_c/mV	Corr. rate/μm/Y
Cu–Al–5Ni	−318	12.0	60	−110	139
Cu–Al–10Ni	−322	10.2	67	−121	118
Cu–Al–30Ni	−418	3.3	106	−65	38
Cu–Al–45Ni	−455	1.6	80	−34	18

The corrosion and passivation behavior of the Cu–Al–Ni alloys can be explained on the basis of the data reported on Cu and those of cast nickel-aluminum bronze [2,4,5,10,26,28]. The major anodic process is the copper dissolution according to equation (3). The cathodic process is actually the oxygen reduction according to:

$$O_2 + 2H_2O + 4e^- \rightarrow 4OH^- \ [E^\circ = 0.401 \text{ V vs SHE}] \quad (5)$$

The decrease in the corrosion rate is due to the formation of the passive Cu_2O layer according to equation (4). In the ternary Al containing alloys an additional passivation process is taking place in neutral solutions in which a layer of Al-oxide is formed as a result of the surface dissolution of Al according to:

$$Al + 4Cl^- \rightarrow AlCl^-_4 + 3e^- \quad (6)$$

$$AlCl^-_4 + 2H_2O \rightarrow Al_2O_3 + 3H^+ + 4Cl^- \quad (7)$$

The remarkably high corrosion resistance of the Cu–Al–Ni alloys is essentially due to the presence of a protective layer of duplex nature containing both Cu_2O and Al_2O_3 [20,22,29]. The

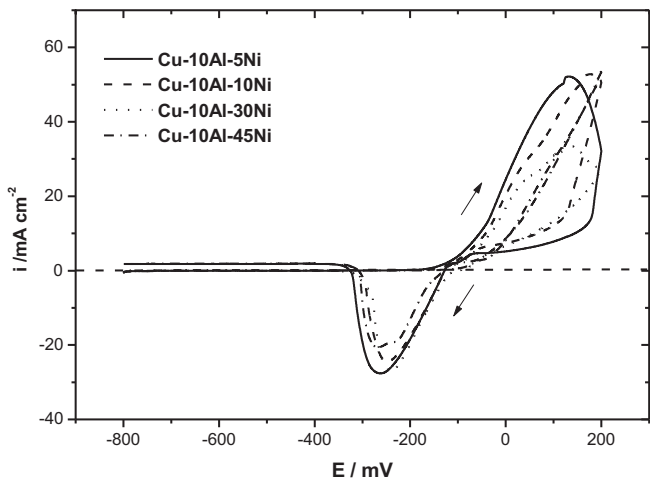

Fig. 2. Cyclic voltammograms of the Cu–Al–Ni alloys, with different Ni contents, in stagnant naturally aerated 0.6 mol dm^{-3} chloride solution of pH 7.0 at 25 °C and scan rate 10 mV s^{-1}.

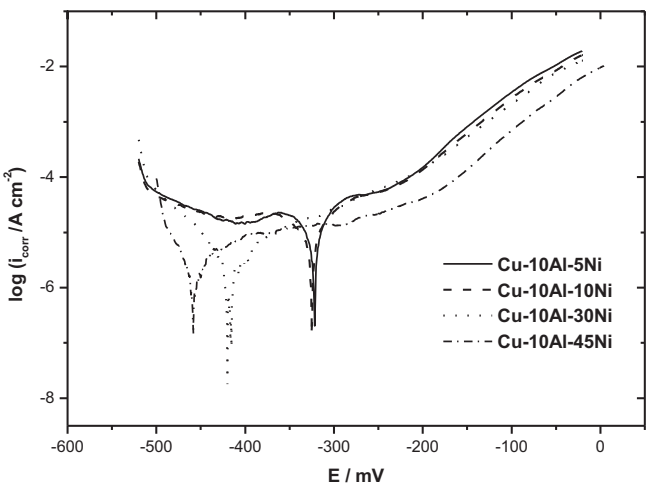

Fig. 3. Potentiodynamic polarization curves of the different Cu–Al–Ni alloys in stagnant naturally aerated 0.6 mol dm^{-3} chloride solution of pH 7.0 at 25 °C and scan rate 5 mV s^{-1}.

Please cite this article in press as: H. Nady, et al., The role of Ni content on the stability of Cu–Al–Ni ternary alloy in neutral chloride solutions, Materials Chemistry and Physics (2012), doi:10.1016/j.matchemphys.2012.03.096

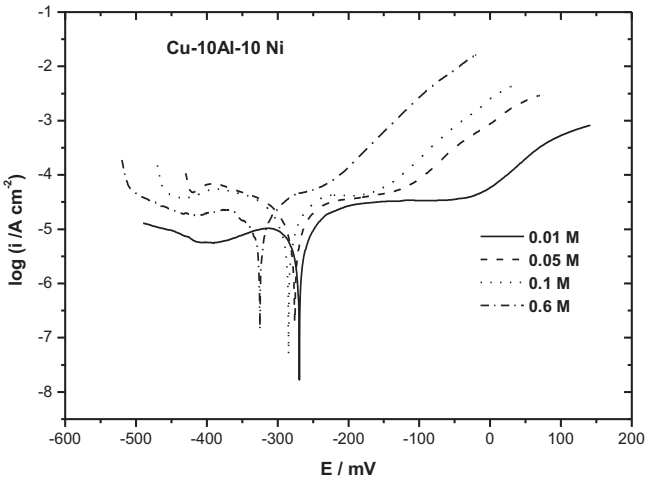

Fig. 4. Potentiodynamic polarization curves of the Cu−10Al−10Ni alloy in stagnant naturally aerated chloride solutions of different concentration at 25 °C and scan rate 5 mV s^{-1}.

Table 3
Potentiodynamic polarization parameters of different Cu−Al−Ni alloys after 1 h of alloy immersion in stagnant naturally aerated neutral chloride solutions of different concentrations at 25 °C.

Alloys	Cl^-/mol dm^{-3}	E_{corr}/mV	i_{corr}/μAcm^{-2}	$ß_a$/mV	$ß_c$/mV	Corr. rate/μm/Y
Cu−Al−5Ni	0.01	−251	12	208	−117	135
	0.05	−277	18	207	−143	205
	0.1	−298	22	160	−192	254
	0.6	−318	12	60	−110	139
	1.0	−405	3.5	60	−80	40
Cu−Al−10Ni	0.01	−337	3.1	66	−40	36
	0.05	−274	18	200	−157	203
	0.1	−282	15	119	−125	177
	0.6	−322	10.2	67	−121	118
	1.0	−377	2	56	−66	24
Cu−Al−30Ni	0.01	−272	5	129	−182	60
	0.05	−270	8	118	−70	93
	0.1	−282	9	122	−107	99
	0.6	−418	3.3	106	−65	38
	1.0	−430	2.8	80	−61	33
Cu−Al−45Ni	0.01	−184	0.6	70	−40	7
	0.05	−379	0.74	40	−15	9
	0.1	−429	0.7	23	−6	8
	0.6	−455	1.6	80	−34	18
	1.0	−492	2.0	105	−31	23

inner layer is an Al-rich barrier layer which is impermeable to Cu (I) cations preventing the dissolution of Cu from the alloy surface. The outer layer is a porous Cu-rich consisting mainly of Cu_2O passive film [29,30]. This result was confirmed by EDX, where the surface shows higher concentration of Cu and also lower concentration of Ni due to Ni diffusion in the inner barrier layer. Al is involved in the compact inner layer and its concentration on the surface is slightly lower than the bulk. The duplex barrier layer inhibits the ionic transport and hence an increased corrosion resistance can be recorded. The increase of the Ni content in the alloy with the constant Al ratio leads to enrichment of Ni to the surface. Thus, the number of cation vacancies that normally exist in Cu (I) oxide is reduced and the passivity of the alloy surface increases [11,22].

The effect of chloride ions on the corrosion behavior of the different alloys was investigated. Typical potentiodynamic polarization curves of the Cu−10Al−10Ni are presented in Fig. 4. The other investigated alloys show almost the same behavior and the presence of relatively higher iron ratio ($\cong$2.2%) in the low Ni content alloys did not affect the general behavior of the alloy. The corrosion parameters of the investigated alloys in the different chloride solutions were calculated from the corresponding potentiodynamic data and presented in Table 3. The general trend is the increase of the corrosion current density with the increase of chloride ion up to ($[Cl^-]$ = 0.1 mol dm^{-3}). At higher chloride ion concentrations a decrease in the corrosion current density was recorded. The sharp increase and also the decrease of the corrosion rate are dependent on the Ni content. For alloys of $\geq$30% Ni a relatively low corrosion rate was recorded. Such a behavior can be attributed to the loading of the alloy surface with Ni at higher Ni contents, which prevents the Cu dissolution in the early stages of the alloy immersion in solutions with lower chloride ion concentrations. Increasing the Cl^- concentration leads to the attack of the adsorbed insoluble CuCl layer to form the soluble $CuCl_2^-$ species and an increase in the corrosion rate could be recorded. At concentrations ($[Cl^-] > 0.1$ mol dm^{-3}), the soluble $CuCl_2^-$ hydrolyzes to form a passive Cu_2O layer together with the possibility of Al_2O_3 formation according to equations (6) and (7) leading to a remarkable decrease in the corrosion rate [25,31].

3.4. EIS investigations

The electrochemical impedance spectra for the different alloys were recorded after different time intervals of the alloy immersion in the stagnant naturally aerated neutral 0.6 mol dm^{-3} chloride solution at open-circuit potential. Representative data of these measurements for the Cu−10Al−45Ni alloy are presented as Bode and Nyquist plots in Fig. 5a and Fig. 5b, respectively. The general trend with all investigated alloys is the increase of the total impedance, Z, with the increase of immersion time. The main feature of all impedance spectra is the presence of a depressed capacitive loop at intermediate frequencies and a single semicircle in Nyquist plot (cf. Fig. 5b). This behavior is attributed to a single time constant comprising relaxation effects due to the surface adsorption processes [20,30,32]. The increase of electrode impedance and of course the diameter of the semicircles of the Nyquist plots means an increase in the charge transfer resistance of the surface oxide film i.e. the corrosion resistance of the alloy with the immersion time. The increase of the phase angle and broadening of the log f vs. phase angle diagram of the Bode plot with the immersion time indicates a decrease in the corrosion rate of the alloys [32].

The impedance data were analyzed using software provided with the impedance system where the dispersion formula (equation (8)) was used. For a simple equivalent circuit model consisting of a parallel combination of a capacitor, C_{dl}, and a resistor, R_p, in series with a resistor, R_s, representing the solution resistance, the electrode impedance, Z, is represented by the mathematical formulation:

$$Z = R_s + \left[R_{ct}/\left\{1 + (2\pi f\, R_{ct}\, C_{dl})^{\alpha}\right\}\right] \quad (8)$$

where α denotes an empirical parameter ($0 \leq \alpha \leq 1$) and f is the frequency in Hz. This formula takes into account the deviation from the ideal RC-behavior in terms of a distribution of time constants due to surface inhomogeneties, roughness effects, and variations in properties or compositions of surface layers [33,34]. The experimental impedance data were fitted to theoretical data according to the simple equivalent circuit model shown in Fig. 5c. To account for the presence of a passive film, some times it is needed to analyze the impedance data according to more complex equivalent circuit models [20,22,30]. The simple model was found to be enough for these investigations. The procedure of data fitting was carried out for all investigated alloys in the stagnant naturally aerated neutral 0.6 mol dm^{-3} chloride solution and after 1 h of alloy immersion where a steady state is assured. The calculated equivalent circuit

Please cite this article in press as: H. Nady, et al., The role of Ni content on the stability of Cu−Al−Ni ternary alloy in neutral chloride solutions, Materials Chemistry and Physics (2012), doi:10.1016/j.matchemphys.2012.03.096

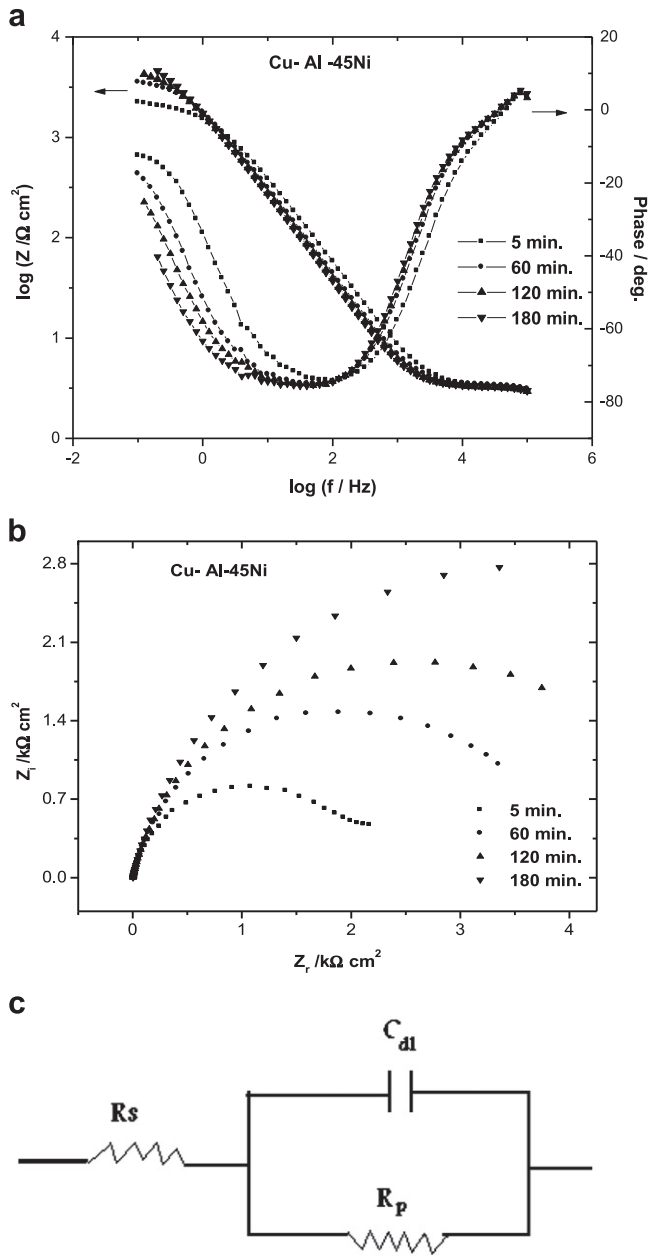

Fig. 5. a: Bode plot of the Cu−10Al−45Ni alloy after different time intervals of alloy immersion in stagnant naturally aerated 0.6 mol dm^{-3} chloride solution of pH 7.0 at 25 °C. b: Nyquist impedance plots of the Cu−10Al−45Ni after different time intervals of alloy immersion in stagnant naturally aerated 0.6 mol dm^{-3} chloride solution of pH 7.0 at 25 °C. c: Equivalent circuit model for the impedance data fitting of the Cu−Al−Ni alloys; R_s = electrolyte resistance, R_p = charge transfer (corrosion) resistance and C_{dl} = electrode capacitance.

parameters are presented in Table 4. The value of R_p of the different alloys increases with the increase in the Ni content and also with the increase of the immersion time, especially for alloys of high Ni content. These results are summarized in Fig. 6. Fig. 6a presents the variation of R_p with the immersion time for the different alloys, whereas Fig. 6b presents clearly the approximate linear increase of R_p with the increase of the Ni content. It is worthwhile to mention that the hump recorded for R_p values of the 45% Ni is correlated with the recorded open-circuit potential variation of the same alloy with time. The recorded high corrosion resistance values at higher Ni content can be attributed to the formation of a uniform passive layer on the alloy surface that is related to the complex

Table 4
Equivalent circuit parameters for the different Cu−Al−Ni alloys after 1 h of alloy immersion in stagnant naturally aerated 0.60 mol dm^{-3} chloride solution of pH 7.0 at 25 °C.

Alloys	R_s/Ω	R_p/kΩ cm^2	C_{dl}/μF cm^{-2}	α
Cu−Al−5Ni	1.2	1.39	457	0.99
Cu−Al−10Ni	0.3	1.60	498	0.99
Cu−Al−30Ni	0.4	3.26	154	0.99
Cu−Al−45Ni	0.9	3.96	80	0.99

metallurgical structure of alloys of Ni content higher than 30%. The surface morphology of these specimens were smooth and did not show any flawed regions even after 24 h of electrode immersion in the chloride containing solution. The calculated value of α is approximately 1, which means that the barrier layer is behaving like an ideal capacitor [33,34].

The effect of chloride ion concentration on the behavior of the ternary alloy with different Ni content after 1 h of electrode immersion can be seen clearly from the values presented in Table 5.

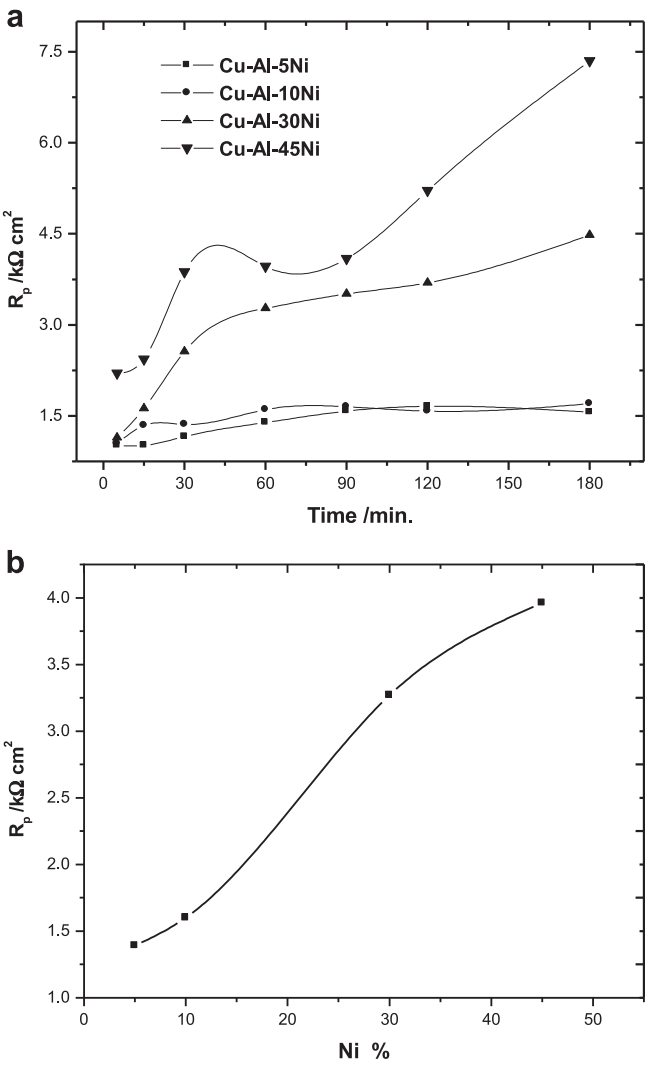

Fig. 6. a: Variation of the corrosion resistance of the barrier layer on the different Cu−Al−Ni alloys with the time of immersion in stagnant naturally aerated 0.6 mol dm^{-3} chloride solutions of pH 7.0 at 25 °C. b: Variation of the corrosion resistance of the barrier layer on the Cu−Al−Ni alloys with the Ni content after 1 h immersion in stagnant naturally aerated 0.6 mol dm^{-3} chloride solutions of pH 7.0 at 25 °C.

Please cite this article in press as: H. Nady, et al., The role of Ni content on the stability of Cu−Al−Ni ternary alloy in neutral chloride solutions, Materials Chemistry and Physics (2012), doi:10.1016/j.matchemphys.2012.03.096

Table 5
Equivalent circuit parameters for the different Cu–Al–Ni alloys after 1 h of alloy immersion in stagnant naturally aerated neutral chloride solutions of different concentrations at 25 °C.

Alloys	Cl^-/M	R_s/Ω	R_p/kΩ cm^2	C_{dl}/μF cm^{-2}	α
Cu–Al–5Ni	0.01	29.2	10.01	127.1	0.99
	0.05	24.6	5.31	119.8	0.99
	0.1	12.5	6.07	65.6	1.0
	1.0	0.1	0.99	402.9	0.99
Cu–Al–10Ni	0.01	33.6	9.12	87.3	0.99
	0.05	25.3	8.22	77.4	0.99
	0.1	14.0	6.21	102.5	1.0
	1.0	0.3	1.04	306.3	0.99
Cu–Al–30Ni	0.01	34.3	8.48	93.8	0.99
	0.05	20.6	5.59	142.2	0.99
	0.1	9.5	4.97	160.2	0.99
	1.0	0.1	2.39	166.4	1.0
Cu–Al–45Ni	0.01	21.9	25.22	50.5	0.99
	0.05	18.6	10.17	78.2	0.99
	0.1	8.2	6.86	92.8	0.99
	1.0	0.9	4.79	83.1	1.0

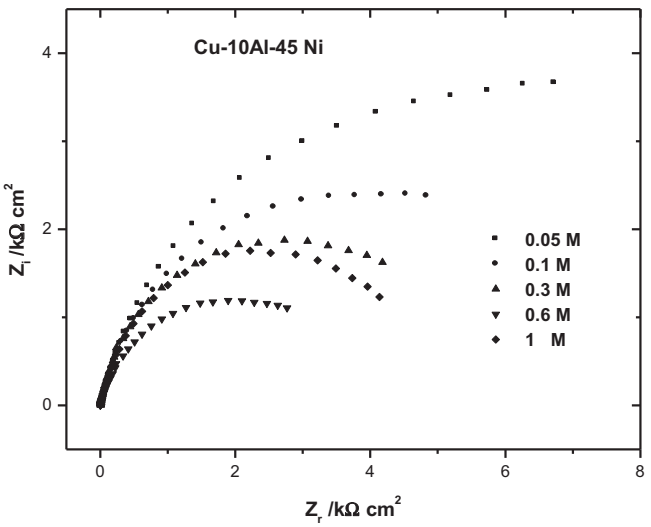

Fig. 7. Nyquist impedance plots of the Cu–10Al–45Ni alloy after 1 h immersion in stagnant naturally aerated chloride solutions of different concentration at pH 7.0 and 25 °C.

A representative Nyquist plot for the Cu–Al–45Ni in solutions of different chloride concentrations is presented in Fig. 7. The resistance of oxide film decrease as the concentration of chloride ion increases which is in good agreement with the potentiodynamic polarization data. The decrease of R_p recorded from the impedance measurements is probably due to the attack of the formed insoluble copper corrosion products (Cu_2O and/or CuCl) during early stages by chloride ions where Cu^+ soluble complexes can be formed [35]. The surface analysis by EDX did not show chloride ions in the barrier layer and is very similar to that obtained in chloride free solutions, which explains why this layer behaves like an ideal capacitor [22].

4. Conclusion

The presence of Al in the ternary Cu–Al–Ni alloy improves its stability due to the formation of the stable Al_2O_3 in the barrier film. The corrosion resistance of the Cu–10Al–*x*Ni alloy in the chloride containing neutral solutions increases with the increase of the Ni content. The high Ni content leads to the enrichment of the surface with Ni, which decreases the vacancies in the Cu (I) oxide and hence increases the corrosion resistance. Prolonged immersion of the alloy in the solution passivates its surface due to the formation of an adherent barrier layer of duplex nature. In all cases the barrier layer behaves like an ideal capacitor.

References

[1] R.W. Cahn, P. Hassen, E.J. Kramer, Materials Science, Technology, a Comprehensive Treatment Structure and Properties of Non Ferrous Alloys, vol. 8, VCH, New York, 1996.
[2] G. Kear, B.D. Barker, K.R. Stokes, F.C. Walsh, J. Appl. Electrochem. 34 (2004) 659.
[3] D.A. Jones, Principles and Prevention of Corrosion, second ed. Prentice Hall, Upper Saddle River, NJ, 1996, p. 518.
[4] G. Kear, B.D. Barker, K.R. Stokes, F.C. Walsh, J. Appl. Electrochem. 34 (2004) 1235.
[5] G. Kear, B.D. Barker, K.R. Stokes, F.C. Walsh, J. Appl. Electrochem. 34 (2004) 1241.
[6] G. Kear, B.D. Barker, K.R. Stokes, F.C. Walsh, Electrochim. Acta 52 (2007) 1889.
[7] G. Kear, B.D. Barker, K.R. Stokes, F.C. Walsh, Electrochim. Acta 52 (2007) 2343.
[8] A. Schussler, H.E. Exner, Corros. Sci. 34 (1993) 1803.
[9] M. Gojic, L. Vrsalovic, S. Kozuh, A. Kneissl, I. Anzel, S. Gudic, B. Kosec, M. Kliskic, J. Alloys Compounds 509 (2011) 9782.
[10] J.C. Scully, The Fundamentals of Corrosion, Pergamon Press, Oxford, 1990.
[11] A. Schussler, H.E. Exner, Corros. Sci. 34 (1993) 1793.
[12] R.F. North, M.J. Pryor, Corros. Sci. 10 (1970) 297.
[13] J.M. Popplewel, R.J. Hart, J.A. Ford, Corros. Sci. 13 (1973) 295.
[14] R.G. Blundy, M.J. Pryor, Corros. Sci. 12 (1972) 65.
[15] H. Shih, H.W. Pickering, J. Electrochem. Soc. 134 (1987) 1949.
[16] W.B. Brooks, Corrosion 24 (1968) 171.
[17] S. Petetin, J. Crousier, J.P. Crousier, Mater. Chem. Phys. 10 (1984) 317.
[18] J. Osterwald, H.H. Uhlig, J. Electrochem. Soc. 108 (1961) 515.
[19] W.A. Badawy, K.M. Ismaila, A.M. Fathi, Electrochim. Acta 50 (2005) 3603.
[20] W.A. Badawy, F.M. Al-Kharafi, A.S. El-Azab, Corros. Sci. 41 (1999) 709.
[21] S.B. Ribotta, L.F. La Morgia, L.M. Gassa, M.E. Folquer, J. Electroanal. Chem. 624 (2008) 262.
[22] W.A. Badawy, M. El-Rabiee, N.H. Hilal, H. Nady, Electrochim. Acta 56 (2010) 913.
[23] J.P. Diard, J.M. Le Canut, B. Le Gorrec, C. Montella, Electrochim. Acta 43 (1998) 2469.
[24] F.K. Crundwell, Electrochim. Acta 36 (1991) 2135.
[25] A.L. Bacarella, J.C. Griess, J. Electrochem. Soc. 120 (1973) 459.
[26] C. Deslouis, B. Tribollet, G. Mengoli, M.M. Musiani, J. Appl. Electrochim. 18 (1988) 374.
[27] G.D. Sulka, P. Jozwik, Intermetallics 19 (2011) 974.
[28] G. Kear, B.D. Barker, F.C. Walsh, Corros. Sci. 46 (2004) 109.
[29] J.A. Wharton, R.C. Barik, G. Kear, R.J.K. Wood, K.R. Stokes, F.C. Walsh, Corros. Sci. 47 (2005) 3336.
[30] W.A. Badawy, M. El-Rabiee, N.H. Hilal, H. Nady, Electrochim. Acta 55 (2010) 1880.
[31] K.D. Efird, Corrosion 31 (1975) 77.
[32] W.A. Badawy, S.S. El-Egamy, K.M. Ismail, Br. Corr. J. 28 (1993) 133.
[33] K. Hladky, L.M. Calow, J.L. Dawson, Br. Corr. J. 15 (1980) 20.
[34] J. Hitzig, J. Titz, K. Juettner, W.J. Lorenz, E. Schmidt, Electrochim. Acta 29 (1984) 287.
[35] K. Nobe, G.L. Bauerle, Corrosion 37 (1981) 426.

Please cite this article in press as: H. Nady, et al., The role of Ni content on the stability of Cu–Al–Ni ternary alloy in neutral chloride solutions, Materials Chemistry and Physics (2012), doi:10.1016/j.matchemphys.2012.03.096